Stabilization of linear ion beam right-hand polarized instabilities by nonlinear Alfvén/ion-cyclotron waves

L. Gomberoff

Departamento de Física, Facultad de Ciencias, Universidad de Chile, Santiago, Chile

Received 9 January 2003; revised 3 March 2003; accepted 14 March 2003; published 27 June 2003.

[1] It is shown that ion-beam plasma electromagnetic right-hand polarized instabilities can be stabilized by nonlinear left-hand polarized waves. This phenomenon constitutes a nonlinear saturation mechanism for right-hand polarized instabilities. Complete stabilization occurs for left-hand wave amplitudes above a threshold value. The saturation mechanism takes place within a large range of pump wave frequencies and plasma temperatures. *INDEX TERMS:* 7839 Space Plasma Physics: Nonlinear phenomena; 7868 Space Plasma Physics: Wave/wave interactions; 7871 Space Plasma Physics: Waves and instabilities; 7827 Space Plasma Physics: Kinetic and MHD theory; 7899 Space Plasma Physics: General or miscellaneous; *KEYWORDS:* right-hand polarization, linear instabilities, left-hand polarization, nonlinear saturation

Citation: Gomberoff, L., Stabilization of linear ion beam right-hand polarized instabilities by nonlinear Alfvén/ion-cyclotron waves, *J. Geophys. Res.*, *108*(A6), 1261, doi:10.1029/2003JA009837, 2003.

1. Introduction

[2] Electromagnetic ion beam-plasma interactions take place in several space and astrophysics environments as well as in laboratory plasmas. In the linear theory these waves have been studied both numerically and analytically [see, e.g., *Gary*, 1991; *Gomberoff and Elgueta*, 1991; *Gnavi et al.*, 1996; *Gomberoff et al.*, 1996; *Gomberoff and Astudillo*, 1998; *Gomberoff et al.*, 2000].

[3] Nonlinear behavior of left-hand polarized electromagnetic waves in a solar wind-like plasma involving alpha particles drifting relative to the proton, have been studied by *Hollweg et al.* [1993] and *Gomberoff et al.* [1994]. Studies of parametric decays of right-hand waves have been carried out by *Hollweg* [1994] [see also *Jayanti and Hollweg*, 1994a, 1994b]. Their nonlinear evolution has also been studied by using drift kinetic effects [*Inhester*, 1990], and hybrid computer simulation techniques [*Vasquez*, 1995]. Studies including dissipation effects have been carried out by *Gomberoff et al.* [2000, 2001]. The effect and evolution of the beam for right and left hand polarized waves, have also been studied by using simulation experiments [see, e.g., *Daughton et al.*, 1999]. The effect of varying beam speed on the parametric decays of right-hand polarized waves have been recently considered by *Gomberoff et al.* [2002].

[4] In this paper a new phenomenon is investigated. It consists of the stabilization of linear right-hand polarized instabilities due to nonlinear left-hand polarized waves. It is a saturation mechanism of right-hand polarized ion-beam induced instabilities. As Alfvén or ion-cyclotron waves grow, they can stabilize the linear right-hand instability triggered by an ion beam. Apart from being an interesting effect in itself, this saturation process may be important in the understanding of processes in space plasma regions where right-hand polarized beam-plasma instabilities are active or in regions where large amplitude Alfvén or ion-cyclotron waves are observed to coexist with ion beams.

[5] The paper is organized as follows. In section 2 the linear electromagnetic beam plasma dispersion relation in the semicold approximation is briefly discussed. In section 3 a brief derivation of the nonlinear dispersion relation is presented. The dispersion relation is then solved graphically in order to illustrate the saturation mechanism. In section 4 the results are discussed.

2. Linear Dispersion Relation

[6] The plasma dispersion for polarized electromagnetic waves propagating in the direction of an external magnetic field, in a system consisting of electrons, a proton core, and a proton beam is given by [*Gomberoff*, 1992; *Gomberoff and Hernández*, 1992; *Gnavi et al.*, 1996; *Gomberoff and Astudillo*, 1996],

$$y_0^2 = \frac{x_0^2}{1 - x_0} + \frac{\eta(x_0 - y_0 U)^2}{1 - (x_0 - y_0 U)}. \qquad (1)$$

where $x_0 = \omega_0/\Omega_p$, $y_0 = k_0 v_A/\Omega_p$, $v_A = B_0/(4\pi n_p M_p)^{1/2}$ is the Alfvén speed, $U = V/v_A$ is the normalized beam velocity, $\eta = n_b/n_c$ is the beam density relative to the core density, and $\Omega_p = qB_0/cM_p$ is the proton gyrofrequency.

[7] The dispersion relation, equation (1), is valid in a current-free plasma and in the reference frame where the proton core is at rest [*Gomberoff and Elgueta*, 1991]. For an alpha particle beam, the dispersion relation was first derived by using kinetic theory in the semi-cold approximation [*Gomberoff and Elgueta*, 1991] and later on by using fluid theory [*Hollweg et al.*, 1993]. The dispersion relation for an arbitrary ion beam is given by *Gomberoff* [1992].

[8] In Figure 1 the dispersion relation given by equation (1) is shown for $U = 2$ and $\eta = 0.2$. For $\eta = 0.2$ the threshold

Copyright 2003 by the American Geophysical Union.
0148-0227/03/2003JA009837

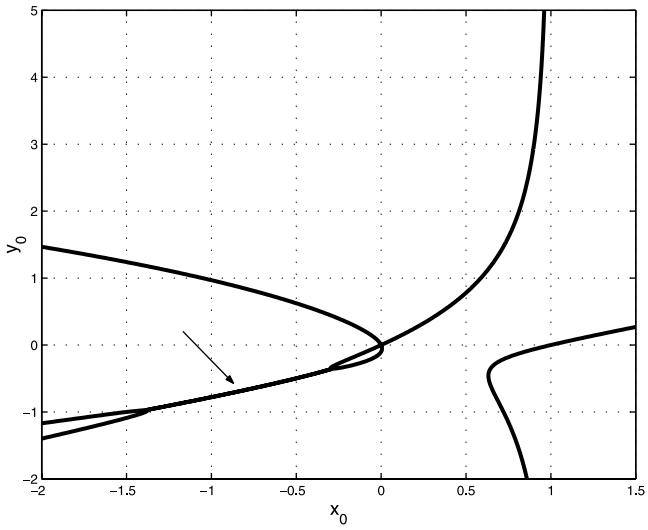

Figure 1. Linear dispersion relation, equation (1), x_0 vs. y_0, for $\eta = 0.2$ and $U = 2$.

for right-hand instabilities is $U \simeq 1.9$ [*Gomberoff and Astudillo*, 1998; *Gomberoff et al.*, 2000]. Proton beams with large drift velocity have been observed in several regions of space [*Hoppe et al.*, 1981, 1982; *Marsch*, 1991; *Gary*, 1991]. The first and fourth quadrant describe the dispersion relation for forward and backward propagating left-hand polarized waves, respectively. The third and second quadrant describe right-hand polarized electromagnetic ion-cyclotron waves propagating forward and backwards, respectively. The line crossing the x-axis at $x = 1$ in the first quadrant is due to the proton beam, and it satisfies $(x_0 - y_0 U) \simeq 1$ (being equal to 1 on the axis, $y_0 = 0$). This branch in the third quadrant has been shown to have negative energy [*Gnavi et al.*, 1996]. The dispersion relation is a third-order polynomial in x_0 and y_0 with real coefficients. Therefore the roots are either real or complex conjugate. The straight line between $-0.3 \geq x_0 \geq -1.4$, in the third quadrant of Figure 1 and indicated by an arrow, is the real part of two complex conjugate roots of equation (1). It corresponds to a right-hand polarized instability for waves moving in the direction of the external magnetic field [*Gomberoff and Astudillo*, 1998; *Gomberoff et al.*, 2000].

3. Nonlinear Dispersion Relation

[9] We now derive very briefly the nonlinear dispersion relation assuming the plasma to be composed by electrons, background protons, beam protons, and a left-hand circularly polarized wave propagating along the external magnetic field. This wave corresponds to the pump wave. Each plasma component satisfies the following fluid equation of motion,

$$\left(\frac{\partial}{\partial t} + u \cdot \nabla\right)\vec{u} = \frac{q_l}{m_l}\left(\vec{E} + \frac{1}{c}\vec{u} \times \vec{B}\right) - \frac{\vec{\nabla} p}{n_l m_l}, \qquad (2)$$

where $\vec{u}$ is the bulk velocity, q_l is the electric charge, m_l is the mass, $\vec{E}$ and $\vec{B}$ are the electric and magnetic field respectively, and p is the pressure.

[10] As pointed out before, the dispersion relation given by equation (1) was first derived by linearizing Vlasov's equation [*Gomberoff and Elgueta*, 1991] and using the semicold approximation. Later on, it was derived by using first order perturbation theory on the fluid equation (2) for zero temperature [*Hollweg et al.*, 1993]. Finally, it was also shown to be an exact solution of equation (1) for zero pressure [*Gomberoff et al.*, 1994].

[11] In order to derive the nonlinear dispersion relation, we follow a similar procedure to *Hollweg et al.* [1993] [see also *Gomberoff et al.*, 1994, 1995, 1996]. Thus we perturb the fluid equations (2) including the left-hand polarized electromagnetic wave moving in the direction of the external magnetic field along the x-axis, as follows,

$$\begin{aligned} \delta u_x &= Re[u \exp(ikx - i\omega t] \\ \delta E_x &= Re[\epsilon exp(ikx - i\omega t) \\ \delta n_p &= n_0 Re\left[\frac{uk}{\omega - kV_{0x}} \exp(ikx - i\omega t)\right], \end{aligned} \qquad (3)$$

where $V_{0x} = V$ is the beam speed.

[12] For quantities perpendicular to the external magnetic field we write,

$$\begin{aligned} \delta u_\perp &= u_+ \exp(ik_+ x - i\omega_+ t) + u_- \exp(ik_- x - i\omega_- t \\ \delta B_\perp &= b_+ \exp(ik_+ x - i\omega_+ t) + b_- \exp(ik_- x - i\omega_- t) \\ \delta j_\perp &= j_+ \exp(ik_+ x - i\omega_+ t) + j_- \exp(ik_- x - i\omega_- t), \end{aligned} \qquad (4)$$

where $u_\perp = u_y + iu_z$, and similarly for $B_\perp$ and $j_\perp$. On the other hand, $k_\pm = k_0 \pm k$ and $\omega_\pm = \omega_0 \pm \omega$, where k_0 and ω_0 are the frequency and wavenumber of the pump wave, which satisfies the dispersion relation shown in the first quadrant of Figure 1.

[13] Linearizing equation (2) by replacing the perturbed quantities given by equations (3) and (4) upon elimination of all Fourier coefficients appearing in these equations, using also the resonance conditions and taking the electrons to be massless, we obtain the nonlinear dispersion relation [*Gomberoff et al.*, 2002]

$$\begin{aligned} &L_+ L_- D + L_+ R_- B_{-cc} + L_+ R_{-b} B_{-ccb} + L_- R_+ B_+ + L_- R_{+b} B_{+b} \\ &\quad + (B_{-cc} B_{+b} - B_{-ccb} B_+)(R_- R_{+b} - R_{-b} R_+)/D = 0 \end{aligned} \qquad (5)$$

In the last equation,

$$\begin{aligned} L_\pm &= y_\pm^2 - x_\pm^2/\psi_\pm - \eta x_\pm^2/\psi_{\pm b} \\ R_\pm &= y_\pm\left(x_0 - \frac{yx_0^2}{y_0 x} + \frac{x_\pm}{\psi_\pm}\right)/2\psi_0 \\ R_{\pm b} &= \eta y_\pm\left(x_{0b} - \frac{yx_{0b}^2}{y_0 x_b} + \frac{x_{\pm b}}{\psi_{\pm b}}\right)/\psi_{0b} \\ D &= \beta_e' \Delta \eta r_b x^2 + \beta_e' \Delta_b r x_b^2 - \Delta\Delta_b (x x_b)^2 \\ B_+ &= -\beta_e' B_{+b1} \eta r \beta_b x x_b + B_{+1} x^2 (\beta_e' \eta r_b - \Delta_b x_b^2) \\ B_{+b} &= -\beta_e' B_{+1} r_b x x_b + B_{+b} x_b^2 (\beta_e' r - \Delta x^2) \\ B_{-cc} &= -\beta_e' B_{-ccb1} \eta r_b x x_b + B_{-cc1} x^2 (\beta_e' r_b - \Delta_b x_b^2) \\ B_{-ccb} &= -\beta_e' B_{-cc1} r_b x x_b + B_{-ccb1} x_b^2 (\beta_e' r - \Delta x^2) \end{aligned}$$

$$B_{+(b)1} = -\frac{A\psi_{(b)}\left(y_+\psi_{+(b)}x_{0(b)}^2 - y_0\psi_{0(b)}x_{+(b)}\right)}{y_0 y_+ x_{(b)}}$$

$$B_{-cc(b)1} = \frac{A\psi_{+(b)}\left(y_-\psi_{-(b)}x_{0(b)}^2 - y_0\psi_{0(b)}x_{-(b)}^2\right)}{y_0 y_- x_{(b)}}$$

$$\Delta = A + r(1 - \beta_p y^2/x^2)$$

$$\Delta_b = A + r_b\left(1 - \frac{\beta_b y^2}{x_b^2}\right)$$

$$\beta_l = 4\pi n_p \gamma K T_l / B_0^2 \ (l = e, c, b)$$

where $x = \omega/\Omega_p$, $y = kv_A/\Omega_p$, K is the Boltzmann constant, T_l is the temperature of species l, and

$$x_b = x - yU$$
$$x_{0b} = x_0 - y_0 U$$
$$A = (B/B_0)^2$$
$$r_{(b)} = \psi_{0(b)}\psi_{+(b)}\psi_{-(b)}$$
$$\psi_0 = 1 - x_0$$
$$\psi_{0b} = 1 - x_{0b}$$
$$\psi_\pm = 1 - x_\pm$$
$$\psi_{\pm b} = 1 - x_{\pm b}$$
$$x_\pm = x_0 \pm x$$
$$y_\pm = y_0 \pm y$$
$$x_{0b} = x_0 - y_0 U$$
$$x_{\pm b} = x_\pm - y_\pm U$$
$$\beta_e' = \beta_e y^2/(1+\eta).$$

[14] These quantities differ slightly from *Hollweg et al.* [1993] because they considered an alpha particle beam, whereas we are considering a proton beam. The differences lie in factors of 2 and 4 in some of the definitions. These are $L_\pm$, $R_{\pm b}$, B_+, B_{-cc}, δ_b, ψ_{0b}, $\psi_{\pm b}$, and β_e'. The general structure of the terms appearing in equation (5) for different types of plasmas is given by *Gomberoff* [1995] and *Galvão et al.* [1996].

[15] The pump wave is characterized by the coordinates x_0 and y_0, and it is at the origin of the (x, y) coordinate system. For zero pump intensity, $A = 0$, equation (5) reduces to $L_+L_-D = 0$. The solution $L_\pm = 0$ corresponds to the dispersion relation of the upper and lower side band waves, respectively. The other solution $D = 0$ corresponds to the sound waves present in the system which, for $\eta \ll 1$, are given by,

$$x \simeq \pm(\beta_e + \beta_p)^{1/2} y \tag{6}$$

$$(x - yU) \simeq \pm(\beta_b)^{1/2} y \tag{7}$$

[16] Equation (6) represents the ordinary ion-acoustic waves propagating forward and backward relative to the proton core, and equation (7) corresponds to ion-acoustic waves, supported mainly by the proton beam. They also move forward and backward but relative to the beam. The solutions of $L_\pm = 0$ give the various branches of the dispersion relation. The crossings between the solutions give the position and nature of the possible wave couplings of the system. The solutions of the nonlinear dispersion relation equation (5) are invariant under a rotation through an angle of 180°. Therefore it is sufficient to analyze the solutions in the upper half $\omega - k$ plane [see, e. g., *Hollweg et al.*, 1993; *Jayanti and Hollweg*, 1994a, 1994b; *Gomberoff et al.*, 1994; *Gomberoff*, 2000; *Gomberoff et al.*, 2001]. Note that for $A = 0$, only the ion-acoustic modes depend on the temperature. Note also that the cold plasma dispersion relation for electromagnetic modes is a good approximation in those region of space where $\beta_{\|i} = v_{th.i}/v_A \ll 1$ ($v_{th.i} = \sqrt{2KT_i/M_i}$ is the thermal velocity of species i). This may happen either for small temperatures, and also for not so small temperatures [see, e. g. *Gomberoff and Neira*, 1983; *Gomberoff*, 1992], or for very large Alfvén velocity relative to the thermal velocity, like, e.g., in coronal holes [see, e.g., *Cranmer*, 2002, *Hollweg and Isenberg*, 2002, and references therein].

[17] In order to study the nonlinear dispersion relation equation (5) we use a graphical method first derived by *Longtin and Sonnerup* [1986]. Thus as an example, in Figure 2a we have plotted equation (5) for $x_0 = 0.1$, $\eta = 0.2$, $U = 2$, $\beta_e = \beta_p = \beta_b = 0.001$, and $A = 0$ (for a discussion of the meaning of equation (5) in the $A = 0$ limit [see, e. g., *Hollweg et al.*, 1993; *Gomberoff et al.*, 1994]. From equation (1) it follows that the corresponding $y_0 = 0.121$. The various lines in Figure 2a correspond to the upper and lower sideband waves and the ion-acoustic modes. In Table 1 we define the meaning of the labels given to the various lines in equation (5). All plus signs refer to upper sideband waves and minus signs to lower sideband waves. As explained before, the upper and lower sideband waves are solutions of $L_\pm = 0$, respectively. On the other hand, the ion-acoustic waves satisfy $D = 0$. The solutions of equations (6) and (7) are denoted by $\pm s$ and $\pm s_b$ and correspond to the ion-acoustic waves carried mainly by the background protons and proton beam, respectively. There are four solutions for $D = 0$. Therefore the dispersion relation given by equation (5) is a 10 degree polynomial. Since the coefficients of the polynomial are real, the roots are either real or complex conjugate. The latter correspond to instabilities. Therefore instabilities appear in the diagram as horizontal gaps. Consequently, the presence of such gaps shows the existence of instabilities. In Figure 2a there is a large gap between two forward propagating lower side band waves ($-$F, $-$b). This gap is indicated with an arrow. Since for $A = 0$ there are no nonlinear instabilities, the gap corresponds to the linear right-hand polarized instability shown in Figure 1. The maximum growth rate of this linear instability is $\gamma_m/\Omega_p \simeq 0.15$. On the other hand, as it is well known [*Hollweg et al.*, 1993], the crossings preserving energy conservation are resonant crossings that for $A > 0$ can lead to instabilities. In fact, in Figure 2b the pump wave amplitude has been raised to $A = 0.1$. One can see that there are a number of instabilities which can be recognized by the formation of horizontal gaps. This is, for example, the case of the gap between $+F$ and $-b$. This gap is denoted by 1 in Figure 2b and corresponds to an essentially electromagnetic parametric instability [*Forslund et al.*, 1972]. Note that the presence of the beam can lead to new parametric instabilities [see, e.g., *Hollweg et al.*, 1993; *Gomberoff et al.*, 1994]. Moreover, it has been shown recently that variations of the beam velocity can trigger new instabilities and/or can stabilize other previously existing ones [*Gomberoff et al.*, 2002]. A

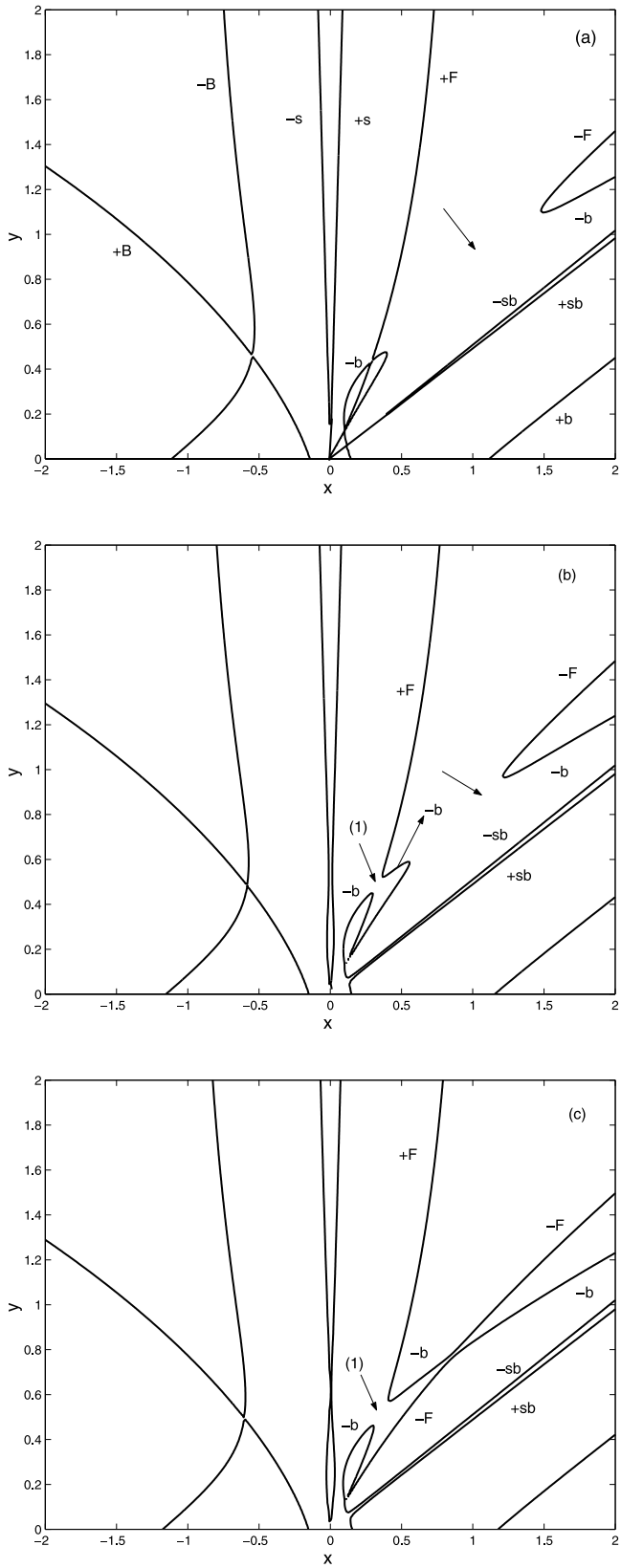

Figure 2. Nonlinear dispersion relation, equation (5), x vs. y, for $x_0 = 0.1$, $\eta = 0.2$, $\beta_e = \beta_p = \beta_b = 0.001$, and several values of A: (a) $A = 0$, (b) $A = 0.1$, and (c) $A = 0.16$.

Table 1. Characterization of the Various Modes Appearing in Equation (5)[a]

Sideband Wave	Polarization
+ (−) F	lh (rh) forward propagating
+ (−) B	rh (lh) backward propagating
+ (−) b	lh (rh) forward propagating
+ (−) s	ion-acoustic forward (backward) propagating
+ (−) s_b	beam-ion-acoustic forward (backward) propagating

[a]The + (−) sign refers to the upper (lower) sideband waves, and lh (rh) refers to left-hand (right-hand) polarization. F refers to the branch of the pump wave (the branch that goes asymptotically to the proton gyrofrequency), and b refers to the branch due to the beam (the branch that satisfies x-yU ≈ 1).

full account of these instabilities including ion-acoustic Landau damping effects will be given somewhere else.

[18] We now study the evolution of the gap shown in Figure 2a as the pump wave amplitude increases. As it follows from Figure 2b, for $A = 0.1$ the gap has become smaller, which means that the instability range has decreased. The maximum growth rate has also decreased to $\gamma_m/\Omega_p \simeq 0.01$. In

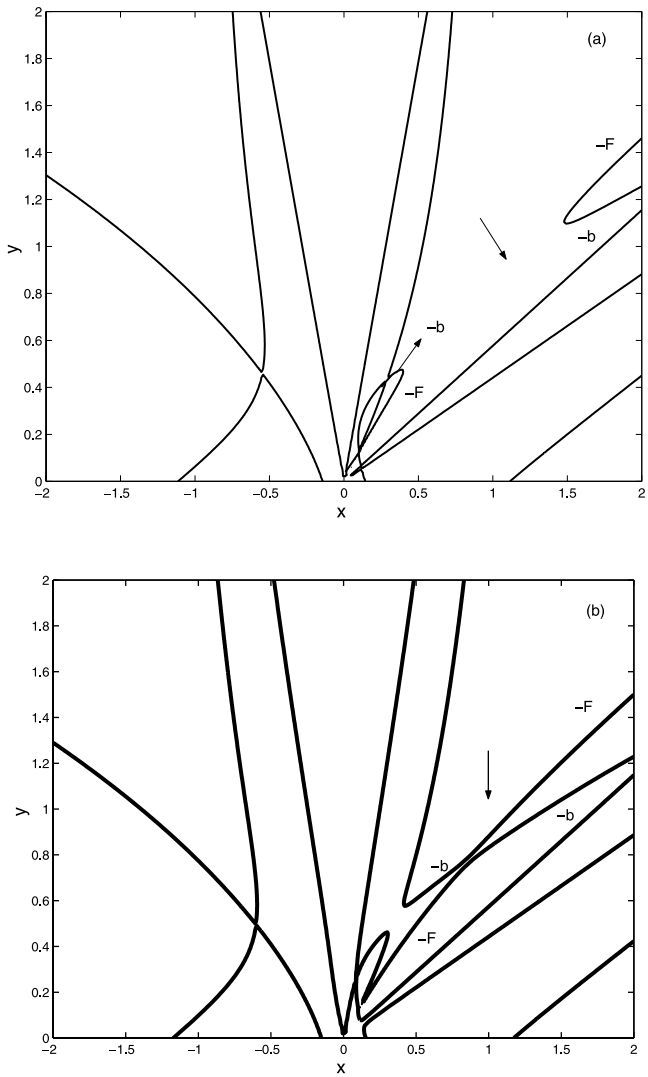

Figure 3. Same as Figure 2 but for $\beta_c = \beta_b = 0.07$, and $\beta_e = 0.001$, for (a) $A = 0$ and (b) $A = 0.15$.

Table 2. Threshold Pump Wave Amplitude, A_t, for Various Pump Wave Frequencies, x_0, and Several β_i Values

X_0	$beta_i$	A_t
0.001	1.0	0.18
	0.3	2.20
	0.1	0.13
	0.01	0.15
	0.001	0.16
0.01	1.0	0.18
	0.3	2.30
	0.1	0.13
	0.01	0.15
	0.001	0.16
0.1	1.0	0.22
	0.3	2.30
	0.1	0.13
	0.01	0.16
	0.001	0.16
0.2	1.0	0.60
	0.3	2.50
	0.1	0.14
	0.01	0.16
	0.001	0.16
0.5	1.0	–
	0.3	2.80
	0.1	0.11
	0.01	0.14
	0.001	0.15
0.7	1.0	–
	0.3	–
	0.1	0.07
	0.01	0.10
	0.001	0.10
0.9	1.0	–
	0.3	–
	0.1	0.01
	0.01	0.04
	0.001	0.04

Figure 2c, A has been further increased to $A = 0.16$. The gap has disappeared altogether implying that the linear stability has been completely stabilized. This occurs for $A \geq 0.16$. The value $A \simeq 0.16$ is the threshold for complete stabilization of the linear right-hand polarized instability.

[19] As a possible application to the solar wind, in Figure 3 we use parameters compatible with the solar wind at 0.3 AU [*Leubner and Viñas*, 1986; *Marsch*, 1991; *Gary*, 1991]. Thus we take $\eta = 0.2$, $\beta_c = \beta_b = 0.07$, $\beta_e = 0.01$ and $x_0 = 0.1$. In Figure 3a we show the dispersion relation, equation (5), for $A = 0$, and in Figure 3b for $A = 0.15$. In the last figure the right-hand instability has been completely stabilized.

4. Discussion

[20] By using a graphical method [*Longtin and Sonnerup*, 1986] we have shown that due to nonlinear effects, a growing Alfvén or ion-cyclotron wave can stabilize linear right-hand polarized instabilities triggered by an ion-beam. In the examples used the pump wave frequency has been chosen to be $x_0 = 0.1$. However, similar results follow for a large range of pump wave frequencies and temperatures, although in some cases stabilization is not possible through this mechanism. In Table 2 the threshold pump wave amplitude, A_t, for complete stabilization of the right-hand instability has been calculated for several pump wave frequencies, x_0, and several β_i-values. As it follows from Table 2, for Alfvén waves, i. e., for frequencies $x_0 \leq 0.1$, the threshold A_t-values range from $0.13 \leq A_t \leq 0.16$ and remain more or less constant for $0.001 \leq \beta_i \leq 1.0$. However, for $\beta_i = 0.3$, $2.20 \leq A_t \leq 2.30$. These values are very large compared to the other cases. In other words there is a range of β_i-values $0.3 \leq \beta_i \leq 0.6$, for which A_t has to be unrealistically large in order to get full stabilization of the right-hand polarized instability. As the pump wave frequency increases to $x_0 = 0.2$, the threshold A_t-values remain almost the same for $0.001 \leq \beta_i \leq 0.1$, but it shows a sharp increase for $\beta_i = 1$. On the other hand, for $x_0 = 0.5$ and $\beta_i = 1$, there is no stabilitzation at all, and again, for $\beta_i = 0.3$, an unrealistic large $A_t = 2.80$-value is required for complete stabilization. In contrast there is only a slight decrease in A_t for $0.001 \leq \beta_i \leq 0.1$ compared with the case when the pump wave frequency corresponds to Alfvén waves. A similar behavior is observed for $x_0 = 0.7$, where again the system remains unstable for $\beta_i = 1$ and $\beta_i = 0.3$. There is however, a sharp decrease of A_t for $0.001 \leq \beta_i \leq 0.1$. Finally, for $x_0 = 0.9$ and $\beta_i = 0.3$ and 1.0, there is no stabilization of the linear instability. However, for $0.001 \leq \beta_i \leq 0.1$, the threshold amplitude continues to decrease to very small values, ranging from 0.01 to 0.04, even at this very large pump wave frequency. The reason why in some cases stabilization is either impossible or it requires unrealistically large A_t values is due to the fact that for large temperatures, the slope of the ion-acoustic sound waves supported mainly by the background protons decreases, forcing the ion-acoustic waves propagating in the direction of the beam to lie within the linear instability region of the dispersion relation. As the pump wave amplitude increases, the ion-acoustic sound waves trigger parametric decays of the pump wave which interfere with the stabilization of the linear instability. In these cases, pitch angle scattering of the beam ions is probably responsible for the saturation of the right-hand instability [see *Daughton et al.*, 1999].

[21] The saturation mechanism discussed here has been derived on the basis of fluid theory. However, as it is well known, when $T_i \geq T_e$, the ion-acoustic modes can be heavily Landau damped. By simulating Landau damping assuming a collisional-like dissipation term in the fluid equations, it has been possible to shown that some parametric decays of a left-hand polarized wave are stabilized, while other frequency regions are actually destabilized [*Gomberoff*, 2000; *Gomberoff et al.*, 2001]. These results have been shown to be in very good agreement with drift kinetic treatments [*Inhester*, 1990] and hybrid simulation results [*Vasquez*, 1995]. The parametric decays that are affected by Landau damping are those decays involving ion-acoustic modes. Since the linear instability has nothing to do with ion-acoustic waves, we do not expect ion Landau damping effects to play a role on the stabilization process.

[22] **Acknowledgments.** This work has been partially supported by FONDECYT grant 1020152.

[23] Shadia Rifai Habbal thanks Venku Jayanti and another referee for their assistance in evaluating this paper.

References

Cranmer, S. R., Coronal holes and the high speed solar wind, *Space Sci. Rev.*, *101*, 229, 2002.

Daughton, W., S. P. Gary, and D. Winske, Electromagnetic proton/proton instabilities in the solar wind: Simulations, *J. Geophys. Res.*, *104*, 4657, 1999.

Forslund, D. W., J. M. Kindel, and E. Lindman, Parametric excitation of electromagnetic waves, *Phys. Rev. Lett.*, *29*, 249, 1972.

Galvão, R. M. O., G. Gnavi, L. Gomberoff, and F. T. Gratton, Parametric decay of shear Alfvén waves in multicomponent plasmas, *Phys Rev. E.*, *54*, 4112, 1996.

Gary, S., Electromagnetic ion/ion instabilities and their consequences in space plasmas: A review, *Space Sci. Rev.*, *56*, 373, 1991.

Gnavi, G., L. Gomberoff, F. T. Gratton, and R. M. O. Galvão, Electromagnetic ion-beam instabilities in a cold plasma, *J. Plasma Phys.*, *55*, 77, 1996.

Gomberoff, K., L. Gomberoff, and H. F. Astudillo, Ion-beam plasma electromagnetic instabilities, *J. Plasma Phys.*, *64*, 75, 2000.

Gomberoff, L., Electrostatic waves in the Earth's magnetotail and in comets, and electromagnetic instabilities in the magnetosphere and the solar wind, *IEEE Trans. Plasma Sci.*, *20*, 843, 1992.

Gomberoff, L., Circularly polarized Alfvén and ion cyclotron waves in space plasmas, *Phys. Script.*, *T60*, 144, 1995.

Gomberoff, L., Ion acoustic damping effects on parametric decays of Alfvén waves, *J. Geophys. Res.*, *105*, 10,509, 2000.

Gomberoff, L., and H. F. Astudillo, Electromagnetic ion-beam plasma instabilities, *Planet. Space Sci.*, *46*, 1683, 1998.

Gomberoff, L., and R. Elgueta, Resonant acceleration of alpha particles by ion cyclotron waves in the solar wind, *J. Geophys. Res.*, *96*, 9801, 1991.

Gomberoff, L., and R. Hernández, On the acceleration of alpha particles in the solar wind, *J. Geophys. Res.*, *37*, 12,113, 1992.

Gomberoff, L., and R. Neira, Convective growth rates of ion cyclotron waves in a $H^+ - He^+$ and $H^+ - He^+ - O^+$ plasma, *J. Geophys. Res.*, *88*, 2170, 1983.

Gomberoff, L., F. T. Gratton, and G. Gnavi, Excitation and parametric decay of electromagnetic ion cyclotron waves in high speed solar wind streams, *J. Geophys. Res.*, *99*, 14,717, 1994.

Gomberoff, L., F. T. Gratton, and G. Gnavi, Nonlinear decay of electromagnetic ion cyclotron waves in the magnetosphere, *J. Geophys. Res.*, *100*, 1871, 1995.

Gomberoff, L., G. Gnavi, and F. T. Gratton, Minor heavy ions beam-plasma interactions in the solar wind, *J. Geophys. Res.*, *101*, 13,571, 1996.

Gomberoff, L., K. Gomberoff, and A. L. Brinca, Ion acoustic damping effects on parametric decays of Alfvén waves: Right-hand polarization, *J. Geophys. Res.*, *106*, 18,713, 2001.

Gomberoff, L., K. Gomberoff, and A. L. Brinca, New parametric decays of proton beam-plasma electromagnetic waves, *J. Geophys. Res.*, *107*(A7), 1123, doi:10.1029/2001JA000265, 2002.

Hollweg, J. V., Beat, modulational, decay instabilities of a circularly polarized Alfvén wave, *J. Geophys. Res.*, *99*, 23,431, 1994.

Hollweg, J. V., and P. A. Isenberg, Generation of the fast solar wind: A review with emphasis on the resonant cyclotron interaction, *J. Geophys. Res.*, *107*(A7), 1147, doi:10.1029/2001JA000270, 2002.

Hollweg, J. V., R. Esser, and V. Jayanti, Modulational and decay instabilities of Alfvén waves: Effect of streaming He^{++}, *J. Geophys. Res.*, *98*, 3491, 1993.

Hoppe, M. M., C. T. Russell, L. A. Frank, T. E. Eastman, and E. W. Greenstadt, Upstream hydromagnetic waves and their association with backstreaming ion population, *J. Geophys. Res.*, *86*, 4471, 1981.

Hoppe, M. M., C. T. Russell, T. E. Eastmann, and L. A. Frank, Characteristics of ULF waves associated with upstream ion beams, *J. Geophys. Res.*, *87*, 643, 1982.

Inhester, B. A., A drift-kinetic treatment of the parametric decay of large amplitude Alfvén waves, *J. Geophys. Res.*, *95*, 10,525, 1990.

Jayanti, V., and J. V. Hollweg, Parametric instabilities of parallel propagating Alfvén waves: Some analytical results, *J. Geophys. Res.*, *98*, 13,247, 1994a.

Jayanti, V., and J. V. Hollweg, On the dispersion relation for parametric instabilities of parallel propagating Alfvén waves, *J. Geophys. Res.*, *19*, 98,049, 1994b.

Leubner, M. D., and A. Viñas, Stability analysis of double picked proton distribution functions in the solar wind, *J. Geophys. Res.*, *91*, 13,366, 1986.

Longtin, M., and B. U. O. Sonnerup, Modulational instability of circularly polarized Alfvén waves, *J. Geophys. Res.*, *91*, 6816, 1986.

Marsch, E., Kinetic theory of the Solar Wind Plasma, in *Physics of the Inner Heliosphere*, edited by E. Marsch and R. S. Shwenn, p. 539, Pergamon, New York, 1991.

Vasquez, V. J., Simulation study of the role of ion-kinetic effects in low frequency wave train evolution, *J. Geophys. Res.*, *100*, 1779, 1995.

L. Gomberoff, Departamento de Fisica, Faculdad de Ciencias, Universidad de Chile, Las Palmeras 3425/Nunoa/Casilla, 653 Santiago, Chile. (lgombero@uchile.cl)